

## VTT Technical Research Centre of Finland

### Bending reliability of screen-printed vias for a flexible energy module

Kujala, Manu; Kololuoma, Terho; Keskinen, Jari; Lupo, Donald; Mäntysalo, Matti; Kraft, Thomas M.

*Published in:*  
npj Flexible Electronics

*DOI:*  
[10.1038/s41528-020-00087-4](https://doi.org/10.1038/s41528-020-00087-4)

Published: 01/12/2020

*Document Version*  
Publisher's final version

*License*  
CC BY

[Link to publication](#)

*Please cite the original version:*

Kujala, M., Kololuoma, T., Keskinen, J., Lupo, D., Mäntysalo, M., & Kraft, T. M. (2020). Bending reliability of screen-printed vias for a flexible energy module. *npj Flexible Electronics*, 4(1), [24].  
<https://doi.org/10.1038/s41528-020-00087-4>



VTT  
<http://www.vtt.fi>  
P.O. box 1000FI-02044 VTT  
Finland

By using VTT's Research Information Portal you are bound by the following Terms & Conditions.

I have read and I understand the following statement:

This document is protected by copyright and other intellectual property rights, and duplication or sale of all or part of any of this document is not permitted, except duplication for research use or educational purposes in electronic or print form. You must obtain permission for any other use. Electronic or print copies may not be offered for sale.

## ARTICLE OPEN



# Bending reliability of screen-printed vias for a flexible energy module

Manu Kujala<sup>1,3</sup>, Terho Kololuoma<sup>1,4</sup>, Jari Keskinen<sup>1,2</sup>, Donald Lupo<sup>1,2</sup>, Matti Mäntysalo<sup>1,2</sup> and Thomas M. Kraft<sup>1,4</sup>✉

The future of printed electronics involves advancements not only related to full system integration, but also lean process manufacturing. A critical aspect of this progress is developed in this study, which evaluates a highly flexible screen printed through-hole-via using silver microparticle inks, for applications in energy harvesting and storage modules. The printed vias' fabrication and durability are evaluated by means of a double sided screen-printing method and repetitive (cyclic) bending tests. Vias, through 125- $\mu\text{m}$ -thick PET foil, were laser cut (nominally 50, 100, 150, and 200  $\mu\text{m}$  diameters) then filled, and simultaneously connected to adjacent vias by screen printing. To investigate the use of the printed via in a monolithic energy module, the vias were used for the fabrication of a flexible printed supercapacitor containing aqueous electrolyte and carbon electrodes. The results indicate that the lower viscosity silver ink (DuPont 5064H) fills the via less effectively than the higher viscosity ink (Asahi LS411AW), and as the via size increases ( $\geq 150$   $\mu\text{m}$  diameter) via walls are coated rather than filled. Conversely, the more viscous ink fills the via thoroughly and exhibited a 100% yield (1010 vias; 100  $\mu\text{m}$  nominal via diameter) with the two-step direct screen-printing method. The 10-mm radius bending test showed no signs of via specific breakdown after 30,000 cycles. The results indicate that this via filling process is likely roll-to-roll compatible to enable multi-layered printed electronic devices.

npj Flexible Electronics (2020)4:24; <https://doi.org/10.1038/s41528-020-00087-4>

## INTRODUCTION

Printed electronics (PE) have provided a means to manufacture electronic devices in a cost-effective and high-volume method utilizing printing techniques such as gravure-, flexo- and screen printing. The additive fabrication method can use relatively low temperatures ( $<150^\circ\text{C}$ ) compared to the conventional silicon based electronics. Moreover, PE enables manufacturing of large area flexible and even stretchable devices; for example, antennas<sup>1</sup>, sensors<sup>2</sup>, thin-film transistors<sup>3,4</sup> and circuits<sup>5</sup>, organic photovoltaics (OPV)<sup>6</sup>, microelectronic packages<sup>7</sup> and on-skin electronics<sup>8</sup> have been demonstrated. The low-cost and high-volume manufacturing becomes more significant as we reach the future Internet of Things (IoT) and Internet of Everything trillion sensor networks, with particular attention on sustainable powering solutions.

Energy-autonomous IoT nodes are a promising prospect receiving increasing interest<sup>9</sup>. The concept of a combined flexible supercapacitor and photovoltaic cell to power an IoT node and facilitate continuous machine-to-machine communication has been proposed and modeled<sup>10</sup>.

OPV modules<sup>6</sup> are printable and potentially low-cost, low toxicity, large area thin-film devices able to harvest energy from light. In OPVs, the absorbing material is a thin layer of organic semiconductor sandwiched between two electrical contacts (commonly a polymer semiconductor: acceptor blend layered between an electron and hole transport layer).

Using primary batteries as an energy storage device often requires replacing the batteries periodically. In applications where long lifetime is needed, the cycle life of secondary batteries may not be long enough. Supercapacitors<sup>11,12</sup>, together with an energy harvesting device such as e.g. photovoltaic cell, can provide long lifetime. Supercapacitors are also able to meet high peak power

requirements of energy storage applications. A supercapacitor consists of two electrodes separated by an ionically conductive electrolyte, with the electrodes typically made of activated carbon.

Our vision is to produce an energy harvesting and storage module (i.e., polymer solar cell and supercapacitor) in a high-volume roll-to-roll process with the interconnection between the components achieved with the screen printed via seen in Fig. 1. As an initial step, the combined structure of a flexible environmentally friendly supercapacitor<sup>13</sup> with the screen printed via, using a completely sealed structure, is evaluated. This evaluation is an elaboration of the initial results and a continuation of the study that examined the use of the printed vias as a viable option<sup>14</sup>.

With multi-layered PE structures, previous studies have shown that a reliable interconnection is achieved by first filling the through-hole vias with dispensed ink and then printing on both sides of the substrate<sup>15–17</sup>. However, this requires at least three print rounds, which increases production time and cost. An advantage with the direct screen-print via filling is to remove the via filling processing step and to avoid an uneven surface on top of the via (caused by via over-fill). The approach in this study is to fill the laser cut via with ink during the two-sided conductive interconnect print process. With the conductive via being made through a flexible substrate, the bending reliability was studied in conjunction to printing. Two different commercially available inks (DuPont 5064H and Asahi LS411AW) and four different laser cut via sizes were investigated (50, 100, 150, and 200  $\mu\text{m}$ ), using a flexible polyethylene terephthalate (PET) substrate. Other similar reliability studies have been done for two-step filled microvias by Péter et. al. The results showed an increase in the via resistance due to crack formation and delamination of ink. Therein, the authors determined that the mechanical stress accumulates on the collar of the via<sup>16</sup>.

<sup>1</sup>Faculty of Computing and Electrical Engineering, Tampere University (formerly Tampere University of Technology), Korkeakoulunkatu 3, FI-33720 Tampere, Finland. <sup>2</sup>Faculty of Information Technology and Communication Sciences, Tampere University, Korkeakoulunkatu 3, Tampere FI-33720, Finland. <sup>3</sup>Present address: Sasken Finland Oy, Vissavedentie 1, FI-69600 Kaustinen, Finland. <sup>4</sup>Present address: VTT Technical Research Centre of Finland Ltd., Kaitoväylä 1, Oulu FI-90590, Finland. ✉email: Thomas.Kraft@vtt.fi

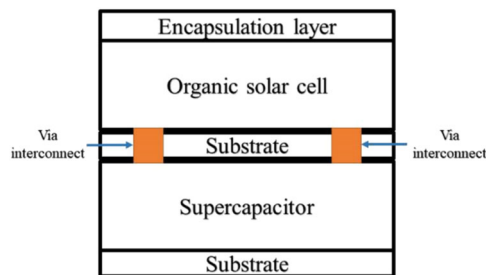


**Fig. 1 Multi-layered energy module.** An energy module using screen-printed vias as the interconnection between energy storage and harvesting components.

## RESULTS AND DISCUSSION

### Optical characterization of laser cut via

Optical characterization results of the vias are shown in Table 1, with nominal via dimensions 50  $\mu\text{m}$  (sample set #1), 100  $\mu\text{m}$  (sample set #2), 150  $\mu\text{m}$  (sample set #3), and 200  $\mu\text{m}$  (sample set #4) wide. As confirmed from the values in Table 1, the laser cut via was cone shaped instead of cylindrical (due to substrate thickness/laser focal point). In all of the cases, difference between top and bottom vias were 54 to 59  $\mu\text{m}$ .

### Via filling characterization results

Following the double sided printing, cross sections of the vias were prepared to evaluate the via filling properties of the inks. Due to the size limitations, sample set #1 had via cross sections cut with a Broad Ion Beam and the image was recorded with a scanning electron microscope (SEM). For the larger via sizes it was possible to use ground resin molds and an optical microscope. The cross section of vias after the printing process is shown in Fig. 2.

In all cases, as seen in Fig. 2, the via is only partially filled during the printing process. However, a reliable electrical connection is still possible. It is also evident that the lower viscosity ink's (DuPont) filling mechanism is less effective than that of the more viscous ink (Asahi). In addition, the inks fill larger via sizes poorly and mainly only coat the via sidewalls. When the ink is on the sidewalls, a less reliable connection was achieved. The reduced reliability is attributed to the top and bottom ink layers not forming a continuous structure inside the via and around the collar.

### Electrical characterization of vias

Electrical conductivity of the ink was measured to ensure reliability of the printing and adequate curing conditions. A four point probe pattern for sheet resistance ( $R_s$ ) was measured with a 10 mA current. Four patterns with 400  $\mu\text{m}$  line widths were printed on the top and bottom of the PET (Supplementary Table 1).

The results indicate that the DuPont ink (mean resistance is 29  $\text{m}\Omega/\square$ ) has a larger deviation in the sheet resistance values compared to the Asahi ink (mean resistance is 25  $\text{m}\Omega/\square$ ). The deviation in resistance illustrates that the print process was not as optimal for the Dupont ink as for the Asahi ink. Fortunately, printing with DuPont did not affect the filling of the via, since the collar size was large enough and was not clogged. However, increased resistance of the DuPont lines may be attributed to the print process as the screen was clogged from some parts of the pattern. With the Asahi ink, the  $R_s$  values are according to datasheet value, which is lower than 40  $\text{m}\Omega/\square$  for 10  $\mu\text{m}$  line thickness. The DuPont inks  $R_s$  value should be less than 14  $\text{m}\Omega/\square$  for 25  $\mu\text{m}$  line thickness.

Electrical characterization results of vias are gathered in Supplementary Table 2, where results show that over 90% of all

**Table 1.** Via diameters.

Sample set	Via size average, top ( $\mu\text{m}$ )	StD ( $\mu\text{m}$ )	Via size average, bottom ( $\mu\text{m}$ )	StD ( $\mu\text{m}$ )	Number of samples, (N)
#1	125	5.9	66	3.9	29
#2	173	7.2	119	2.5	26
#3	232	8.5	172	4.7	24
#4	281	8.2	224	5.0	26

Measured via sizes as compared to the nominal values of 50, 100, 150, and 200  $\mu\text{m}$ .

the vias were considered filled and conducting properly (sample sets 1 (50  $\mu\text{m}$ ), 2 (100  $\mu\text{m}$ ), 3 (150  $\mu\text{m}$ ), and 4 (200  $\mu\text{m}$ )). In most sample sets the yield is over 99%. The best ink filling results were achieved with sample set #2 sample with both inks. Interestingly, sample set #1 had a high number of poor vias compared to failed vias (unlike the fourth set). Conversely, the set #4 had the lowest yield (with both inks) attributed to the reduced aspect ratio causing the ink to escape through the rear of the via rather than fill it. It was noticed that with larger via sizes the ink passes through the via and lays on the screen stage coating the sidewalls of the via instead of filling and creating a reliable plug connector (as seen with the smaller diameters). On the other hand, the smallest via sizes might limit the amount of ink penetration and could explain why samples #2 were most reliable. When comparing the two inks, it is believed that the Asahi fills the via more effectively, since it has higher viscosity (20,000–30,000 cP) than DuPont (10,000–20,000 cP). More modeling of the ink flow and filling of the via could bring essential information in search of the most efficient via diameter and ink combination.

In other scientific papers which have used the two-step filling process, the electrical connection has been 100% or near 100%<sup>16,18</sup>. The resistance of the via is smaller compared to the direct screen-printing via filling method, with the via being filled completely<sup>16</sup>. However, one process step is removed in our direct screen-printing via filling method. A reliable direct screen-printing method has been mentioned by Sven E. Kramer in the book *Printed Circuit Design and Manufacture* by placing a stencil drilled with the same pattern but larger diameters underneath the substrate<sup>19</sup>. The summary of alternative techniques and comparison is shown in Table 2.

### Via-bending results

The reliability of the vias were investigated with the cyclic bending study. The results herein combine an average of the results from three bent daisy-chain structures. An average from the reference samples was also taken from tensile and compressive stressed samples and added to the graphs. The average reference values were taken from four compressive stressed samples and two tensile stressed samples for both inks. Both tensile and compressive stressed reference samples are in the chart to help differentiate the via bending effect from the via-to-via interconnection stress. The daisy-chain samples' resistance change ( $\Delta R$ ) caused from cyclic bending is shown in Fig. 3 for both Asahi and DuPont inks.

The daisy-chain structure faces both compressive and tensile stress and thus is between the reference lines'  $\Delta R$ . The sample lines do still have different  $\Delta R$  when comparing different via sizes, which is caused by the via bending. Looking at Fig. 3a, it is noticed that the largest via sizes are the most resilient to bending with Asahi samples. With DuPont samples (in Fig. 3b) on the other hand, set #2 samples are more resilient to bending compared to set #3 samples. This is likely due to the high starting resistance

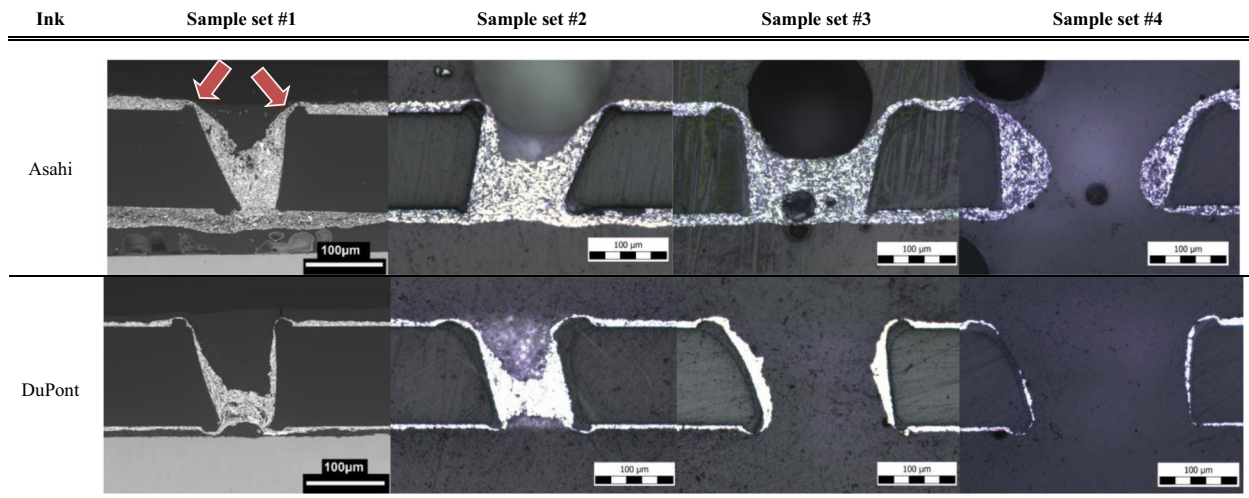


**Fig. 2** **Via cross sections.** Cross section of printed vias using both inks (Asahi and Dupont). Arrows present the via collar, where most of the bending strain was seen to be focused.

**Table 2.** Summary of via filling methods.

Number of processing steps	Via filling method	Via cutting method	Interconnection reliability	Reference
One	Direct screen printing	Punching	Poor (~50%)	Shi et al. <sup>16</sup>
One	Direct screen printing	Laser cutting	Good (99.67%)	Our results
Two	2-step printing method	Punching	Good (almost 100%)	Shi et al. <sup>16</sup>
Two	2-step printing method	Laser cutting	Very good (100%)	Péter et al. <sup>17</sup> Park et al. <sup>15</sup> Lorenz et al. <sup>20</sup>

value of set #3 (set #2  $R_0 = 17.6 \Omega$  and set #3  $R_0 = 20.0 \Omega$ ). Smaller via sizes are thought to have more bending strain on the collar of the via, since the collar area is smaller and larger strain is focused on it. Logically, larger via sizes have larger collars, which is beneficial in terms of the bending strains. Larger via collar equals larger area where the bending strain is focused. This spreads the bending strain and causes smaller resistance change.

In other literature sources the stress hotspots gather around the collar of the via, which correspond to our findings. However, the stress hotspots were also seen on the top of the via, since the ink or conductive adhesive, which is used to fill the via in the two-step filling process, is thicker than the conductive trace<sup>17,20</sup>. Thicker traces face stronger bending strain<sup>21</sup>.

#### Optical characterization of bent vias

SEM images were taken from the bent vias and compared to a non-bent reference sample for the Asahi ink with 100  $\mu\text{m}$  nominal vias. The images were taken on top of the via from the tensile stressed side (Fig. 4).

Increased dissociation of silver microparticles (flakes) around the via collar is caused during bending by the deformation of the PET substrate. The local stretching strain of the collar ink relative to the perpendicularly oriented via induces microcracks around the via cavity. This in turn leads to increased resistance of the via. This observed effect is corroborated by the theoretical modeling performed by Péter et al.<sup>17</sup>.

#### Resistance behavior after bending

After the cyclic bending test, the sample was left on the bending measurement device for a post bending measurement. The resistance value of samples decreased over time, while the samples were left in a non-bent state while connected to the device. The samples' ink polymer matrix relaxes, which brings

the ink's silver flakes closer together. This is seen as a resistance decrease<sup>1</sup>.

To further research the effect of a sample resistance decrease and recovery effect, a cycle-rest-cycle measurement was utilized. In the cycle-rest-cycle measurement, the sample structures faced first ~3000 bend cycles and then left in the straight state for 45 min, then cycled again for 3000 cycles and so forth three times. The cycle-rest-cycle-measurement results are shown in Fig. 5a.

It can be seen from Fig. 5a that the resistance is dropping after the cyclic bending has stopped. However, the resistance quickly returns to the resistance value that it once achieved and starts to rise again when the cycling starts.

An intriguing fact is that the two inks behave differently after the cycling stops. DuPont has a clear slope after the cycling stops and levels relatively fast. However, the Asahi ink's resistance drops almost linearly after the cycling stops.

The resistance recovery of a conductive line was further researched. The resistance change is due to the tensile and compressive stress that the conductor line faces and inadvertently softens the polymer matrix. The polymer and silver flakes were thought to arrange again if the conductor line was annealed again after bending and the ink's polymer compound is then reformed, which makes the silver flakes closer to each other. The hypothesis was then tested with a post anneal test. The samples were bent for 30,000 bending cycles and then left to rest in ambient air for at least 5 days. Then the resistance was again measured after the rest period, annealed for 20 min in a convection oven at 150 or 130  $^{\circ}\text{C}$  for Asahi and DuPont inks respectively. After the post annealing the resistance was measured again. The results from the conductor post anneal test is shown in Fig. 5b. In the post anneal test, it was found that the resistance drops after longer wait periods in ambient air and lowers down considerably after annealing again. This corroborates the starting hypothesis of the polymer matrix reformulating.



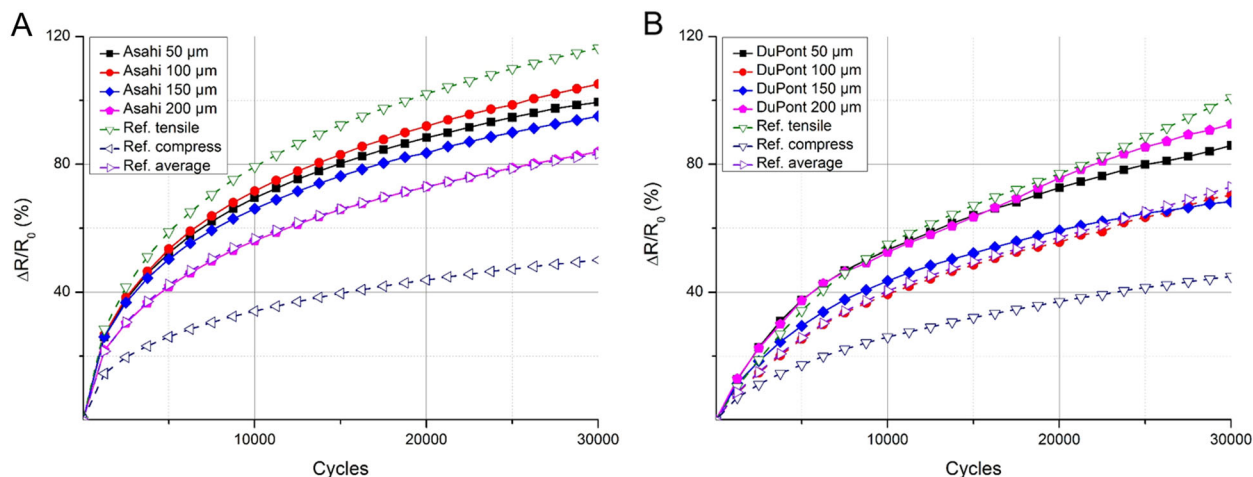


**Fig. 3 Resistance vs. bending cycles.** **a** Asahi samples bending results. Initial resistance ( $R_0$ ) for each case: 50  $\mu\text{m}$ , 13.4  $\Omega$ ; 100  $\mu\text{m}$ , 12.8  $\Omega$ ; 150  $\mu\text{m}$ , 11.9  $\Omega$ ; 200  $\mu\text{m}$ , 11.5  $\Omega$ ; Reference tensile, 10.7  $\Omega$ ; Reference compress 10.5  $\Omega$ . **b** DuPont samples bending results. Initial resistance ( $R_0$ ) for each case: 50  $\mu\text{m}$ , 16.9  $\Omega$ ; 100  $\mu\text{m}$ , 17.6  $\Omega$ ; 150  $\mu\text{m}$ , 20.0  $\Omega$ ; 200  $\mu\text{m}$ , 12.3  $\Omega$ ; Reference tensile, 9.9  $\Omega$ ; Reference compress 15.5  $\Omega$ .

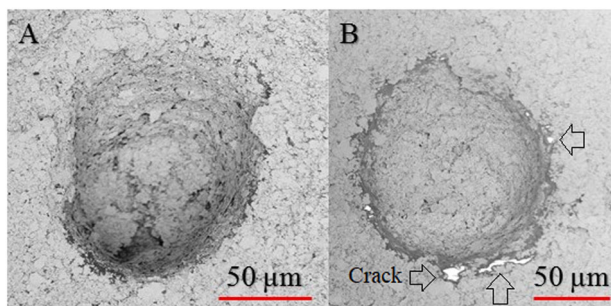


**Fig. 4 Silver ink collar strain.** SEM images of **a** before bent via and **b** after bent via. (sample set #2 via size; 100  $\mu\text{m}$  nominal via diameter, Asahi ink).

When looking at the results from the cycle-rest-cycle measurement, the resistance can rise dramatically when the sample is cyclically bent after rest. The effect of cyclic bending again for a post-annealed sample was then tested. Two rounds of bent daisy-chain sample lines are shown in Fig. 5c, with the first cyclic bent results shown as a comparison.

The bending, after bending and annealing, shows that both of the inks can restore well after cyclic bending. When the sample is cycled again, the resistance does not have the same kind of effect as in the cycle-rest-cycle measurement. However, the ink is not as bendable as before when using the DuPont ink and two of the vias from one of the sample line broke during the measurement. The interconnection starts to break after 8000 bending cycles and breaks completely shortly after the shown 30,000 bending cycles. This could indicate permanent deformations in the ink or cracks in the via collar. The Asahi ink on the other hand restores almost completely to the starting value of the measurement and the resistance change follows the same trend as the first cyclic bending measurement. It seems that the polymer matrix can be restored to its former state before bending if the ink silver particles do not face permanent deformations. The results of bent and annealed samples are gathered in Table 3.

The bending and annealing results show that the first post bend anneal lowers the resistance near to the starting resistance value using Asahi ink. With DuPont the resistance value also lowers, but is clearly higher than the starting value. During the second bending and annealing cycle ("bent twice"), the trend is the same as in the first bend and anneal-cycle, but the resistance does not

drop to the starting resistance value. With DuPont ink, the resistance value rises after each post anneal compared to the starting value. Asahi ink on the other hand recovers completely during the first annealing, but on the second anneal, the resistance is higher compared to the starting value. This case study revealed the curing capabilities of the silver conductor ink. However, consecutive bending might cause permanent deformations in the silver pattern as confirmed in the SEM micrographs of the via collars. Han and Dong have also showed the self-healing capability of a conductor line in their work using molten low melting point metal alloy, and the electrohydrodynamic printing method<sup>22</sup>.

#### Combination of screen printed via and supercapacitor

A supercapacitor was combined with the printed screen-printed through-hole via as a proof of concept. Furthermore, the motivation for this study directly relates to the concept for multi-layered PE components, which can have OPV and energy storage supercapacitors printed in-line on the same base substrate (e.g., Fig. 6c). First, a silver pad was printed on the PET substrate with the supercapacitor's electrode printed on top<sup>13</sup>. The supercapacitor's electrical properties were measured with a Maccor (USA) battery testing device, which charged and discharged the supercapacitor. The supercapacitor's capacitance, equivalent series resistance (ESR), and leakage current were calculated from the measurement data following methods described previously<sup>13,23–24</sup>. Prior bending tests showed 500 cycles with bending radius of 11.5 mm did not impact to the electrical properties of printed supercapacitors<sup>23</sup>. The supercapacitor with vias and a reference supercapacitor structure are shown in Fig. 6.

The measurement results of the reference samples are shown in Table 4, which shows information of the supercapacitors' capacitance, ESR, and leakage current. The results of the measurement correspond to other similar devices in scientific publications<sup>24</sup>. A completely sealed supercapacitor structure can be built with the screen printed via using R2R printing methods, which is illustrated in Fig. 6. Supplementary Fig. 1 shows a picture of the fabricated devices.

The supercapacitors were combined with vias in positive, negative or positive, and negative electrodes. The Asahi and DuPont inks were again compared to each other by creating the supercapacitor and screen printed via structure with both inks. Since the resistance of the vias were not as high as the resistance of the graphite current collector, the silver lines could have

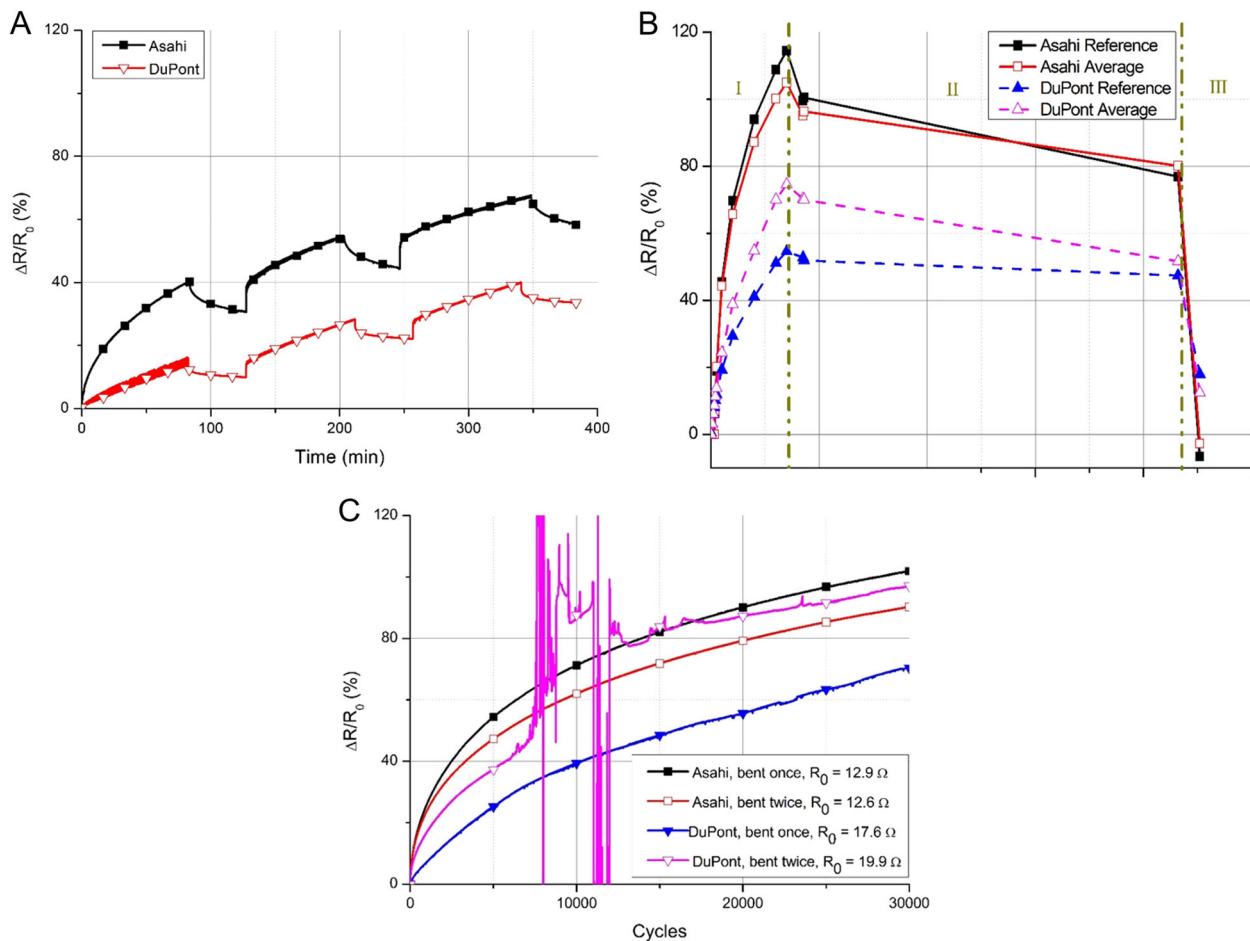


**Fig. 5 Post annealing resistance recovery.** **a** Cycle-rest-cycle measurement results. **b** Post anneal test results. I represents the cycling phase, II waiting phase and III post anneal phase. Inks' increased resistance with bending (I), stable elevated resistance (II), and "healing" with heat treatment (III) clearly visible. **c** Multiple bending cycle trials: bent samples test results with post annealed samples test results. "bent once" correlates with the first bending cycle; "bent twice" refers to samples that have undergone two bending cycles.

**Table 3.** Cyclic bending trials.

Ink	$R_0$ ( $\Omega$ )	After bending 1 ( $\Omega$ )	After anneal 1 ( $\Omega$ )	After bending 2 ( $\Omega$ )	After anneal 2 ( $\Omega$ )
Asahi	13	25.4	12.6	23.1	13.7
DuPont	17.7	29.6	19.6	36.4	26.6

Bent-anneal-bent-anneal resistance measurement results.

multiple vias attached. The results from the supercapacitor and printed through-hole via structure are shown in Table 4.

The comparison of the supercapacitor electrical performance (Table 4) shows that there is little difference in the electrical properties in the via combined structure. However, the ESR values are a few ohms higher in average compared to reference supercapacitors. This is mainly due to the increased resistance of the silver conductor line where the measurement probe is connected.

In conclusion, the screen printed through-hole via filling was evaluated with two different silver inks (with different viscosities) and four different via diameters. The reliability of interconnection between the top and bottom prints were evaluated with a cyclic bending test. The screen printed through-hole via was filled during the screen-printing process. The more viscous Asahi LS411AW ink performed better in the printing process compared

to the DuPont 5064H ink. The Asahi ink's yield of fully functional vias was 99.67% and Dupont's was 95.57%. Four different laser cut via sizes 50, 100, 150, and 200  $\mu\text{m}$  were compared to each other, where the 100  $\mu\text{m}$  had the best yield with both inks. This valuable finding, and associated bending reliability, will be developed and exploited for roll-to-roll multi-sided PE fabrication. Furthermore, for better understanding of the relationship between the ink properties and the via filling process a more detailed, and thorough study is recommended. It would be beneficial to perform such an extensive study to evaluate the ink's via filling properties as ink variables are varied; such as dynamic viscosity, viscous and storage modulus, thixotropicity, as well as the solid load, particle size and the particle shapes of the ink.

In the bending analysis of the screen-printed via, the printed sample structure's resistance of the daisy-chain line was measured, while being cyclically bent 30,000 times. The resistance of a printed line rose in every cyclic bending measurement. However, a via breakdown between the top and bottom side prints was not found in the bending tests. Therefore, bending of the vias has little effect on the overall resistance change in the sample line. However, there seems to be an optimal aspect ratio of vias for filling and bending reliability depending on ink properties.

Ink resistance decreased after the bending was stopped, which is linked to the ink particles rearranging inside the ink and lowering the inks' resistance. However, the ink resistance again rises rapidly, when stressed by bending again. Furthermore, the

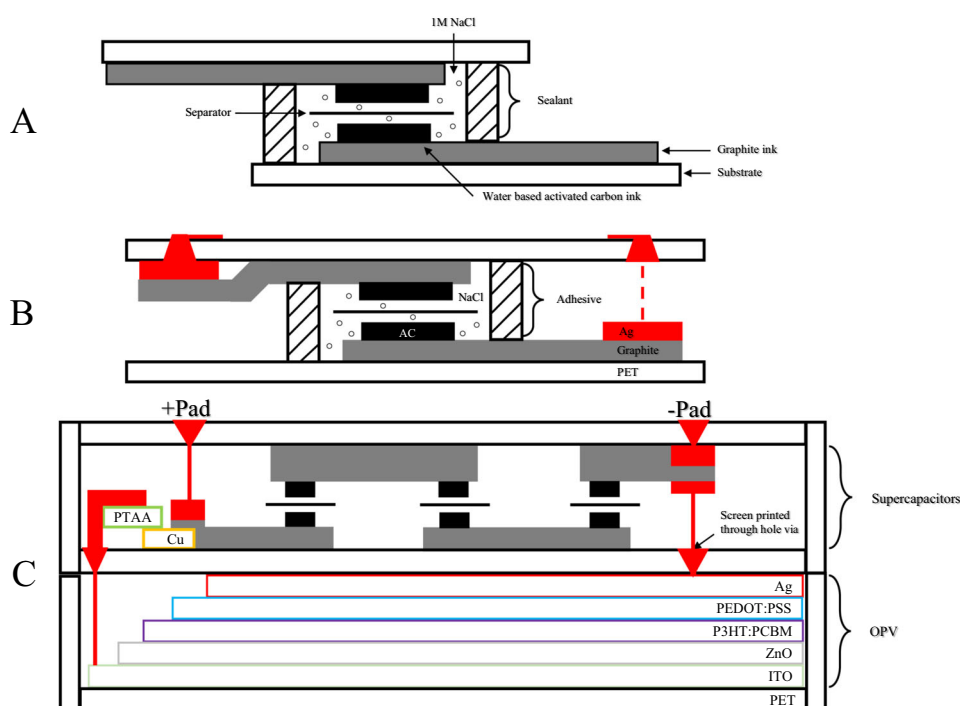


**Fig. 6 Multi-layered component architectures.** **a** Supercapacitor reference structure. **b** Supercapacitor all sealed structure using vias illustrations. **c** Illustration of the vision of OPV and supercapacitor structure.

**Table 4.** Supercapacitor characterization.

Sample (ink)	Capacitance (mF)	ESR ( $\Omega$ )	Leakage current ( $\mu$ A)	Number and location of vias
Reference average	363	21	10	—
Asahi	340	24	10	+ : 1 via
Asahi	385	22	11	— : 1 via
Asahi	336	27	8	+ : 3 vias, — : 1 via
DuPont	372	31	11	+ : 1 via
DuPont	315	16	9	— : 1 via
DuPont	340	22	9	+ : 3 via — : 3 via

Supercapacitor with screen printed via combined structure measurement results. Location of via indicates how many vias does a sample have and which electrode the via or vias are.

inks' resistance substantially reduces when annealed after the bending. The effect is explained as having bending memory, which can be erased when annealed again.

Furthermore, a supercapacitor and a screen-printed through-hole via combined structure was fabricated as an initial step to enable energy module fabrication. The results showed that the screen printed vias and printed interconnects can be used together with the supercapacitor. In the future, the screen printed vias with the direct printing process can be optimized for a R2R fabrication method to print PE devices, such as fully printed energy modules, in a low-cost and high-volume print fabrication line.

## METHODS

### Experimental setup

First, the through-hole vias were in the Melinex ST506 PET substrate (125  $\mu$ m) with a laser beam by Ekspla Atlantic, DPL 015 3 laser (VTT). The laser wavelength was 355 nm, pulse duration 9 ps, repetition range 100–500 kHz with 8 W maximum beam power. The laser's scanner head used a galvanometer driven laser scanning mirror, Intelli SCAN III14. Four

via size sets were cut to the substrate with the laser beam. All substrates were put into an ultrasonic bath for 20–30 min to remove residual PET after laser cutting. After the sonication, all vias were evaluated with an optical microscope Olympus BX51 to determine via diameters and shape.

A direct screen printing approach was utilized to fill the vias with ink during the print process. The silver ink was first printed on the side where the conical via opening was larger (layer 1). Commercially available inks Asahi LS411AW silver paste and DuPont 5064H silver ink were used as the conductive material. The solvent for the inks were butyl cellosolve acetate and isophorone for Asahi and C11-ketone for DuPont. The viscosities were 20,000–30,000 cP and 10,000–20,000 cP for Asahi and DuPont, respectively.

To evaluate the reproducibility of the via filling/printing method, a daisy-chain structure was designed. Each daisy-chain structure had 22 vias in total, with seven daisy-chains placed next to each other on one sample. Along with the daisy chains, each sample had a reference line on the top side. The reference line was printed on one side only (top side) and had no via daisy-chain structure; which provides a reference of the printed conductor without the influence of vias. The screens also had a sample structure, with printed current collector, to combine a supercapacitor with screen printed via.

The supercapacitor's current collector (graphite) was printed on top of a silver pad, which was connected to the screen-printed via. The screen

design for both studies is shown in supplementary information (Supplementary Fig. 2).

A semi-automated flat-bed screen printer (TIC SFC 300 DE from Eickmeyer) was used for printing on the laser cut PET substrates. The screen was ordered from FinnSeri Oy. (Finland) and had a super high modulus polyester monofilament with 79 mesh count per centimeter and 68  $\mu\text{m}$  mesh thickness (with aluminum frame). The screen is both water- and solvent resistant. First, the top side of the pattern was printed (layer 1 in Supplementary Fig. 2C) and then annealed in an oven at 150 °C for 20 min for the Asahi ink and 130 °C for 20 min for the DuPont ink. Subsequently, the bottom side (layer 2 in Supplementary Fig. 2C) of the pattern was printed and sintered in the same conditions as the top print layer.

## Characterization

Supplementary Table 3 summarizes the sample sets that were investigated with over 1000 vias for each of the 8 ink-via combinations (two inks and four via diameters). The resistance of the screen-printed through-hole vias were electrically characterized with a multimeter to determine their degree of connectivity. The resistance of the via was measured to ensure connection from top to bottom of the substrate. The vias were characterized as pass (lower than 1  $\Omega$ ) poor (1 and 10  $\Omega$ ) or failed (over 10  $\Omega$  or open circuit).

In the reliability measurements, samples were placed in a custom made pneumatically controlled bending machine. The machine had two parallel plates and the upper moving plate bends the sample that is attached (bottom stationary). The distance between plates was set to 2 cm (i.e., 10 mm bending radius). The bending device and measurement setup are shown in Supplementary Fig. 3 and had previously been used to investigate the durability of inkjet printed conductors<sup>25</sup>.

An iCraft AD-converter and iPlotter software were used to compile the bend cycle and resistance measurement. Resistance was calculated by feeding 4.92 V across a 1 k $\Omega$  pull-up resistor and the sample line. The sample line's voltage was measured and resistance was calculated with voltage division.

At least 30,000 bending cycles were done in each measurement for samples listed in Supplementary Table 3. Set #1 and #2 were measured twice by mounting the sample facing upside down so that the reference samples undergo both tensile and compressive stress. Tensile and compressive stress locations are illustrated in Supplementary Fig. 3. The bending apparatus is moving and imposes equivalent curved stress on each via twice during a back and forth bending cycle.

## DATA AVAILABILITY

The data that support the findings of this study (and displayed in the figures) are available from the corresponding author upon reasonable request.

Received: 13 February 2020; Accepted: 14 August 2020;

Published online: 18 September 2020

## REFERENCES

- Suikkola, J. et al. Screen-printing fabrication and characterization of stretchable electronics. *Sci. Rep.* **6**, 25784 (2016).
- Xie, L., Feng, Y., Mantysalo, M., Chen, Q. & Zheng, L.-R. Integration of f-MWCNT sensor and printed circuits on paper substrate. *IEEE Sens. J.* **13**, 3948–3956 (2013).
- Noh, Y.-Y., Zhao, N., Caironi, M. & Sirringhaus, H. Downscaling of self-aligned, all-printed polymer thin-film transistors. *Nat. Nanotechnol.* **2**, 784–789 (2007).
- Li, Y. et al. All inkjet-printed metal-oxide thin-film transistor array with good stability and uniformity using surface-energy patterns. *ACS Appl. Mater. Interfaces* **9**, 8194–8200 (2017).
- Chang, J. S., Facchetti, A. F. & Reuss, R. A circuits and systems perspective of organic/printed electronics: review, challenges, and contemporary and emerging design approaches. *IEEE J. Emerg. Sel. Top. Circuits Syst.* **7**, 7–26 (2017).
- Hedley, G. J., Ruseckas, A. & Samuel, I. D. W. Light harvesting for organic photovoltaics. *Chem. Rev.* **117**, 796–837 (2017).
- Khorramdel, B., Torrkeli, A. & Mantysalo, M. Electrical contacts in SOI MEMS using aerosol jet printing. *IEEE J. Electron Devices Soc.* **6**, 34–40 (2018).
- Vuorinen, T., Niittynen, J., Kankkunen, T., Kraft, T. M. & Mantysalo, M. Inkjet-printed graphene/PEDOT:PSS temperature sensors on a skin-conformable polyurethane substrate. *Sci. Rep.* **6**, 35289 (2016).

- Roselli, L. et al. Review of the present technologies concurrently contributing to the implementation of the Internet of Things (IoT) paradigm: RFID, Green Electronics, WPT and Energy Harvesting. In *2015 IEEE Topical Conference on Wireless Sensors and Sensor Networks (WiSNet)* 1–3 (IEEE, 2015).
- Rinne, J., Keskinen, J., Berger, P. R., Lupo, D. & Valkama, M. Feasibility and fundamental limits of energy-harvesting based M2M communications. *Int. J. Wirel. Inf. Netw.* **24**, 291–299 (2017).
- Conway, B. E. *Electrochemical Supercapacitors: Scientific Fundamentals and Technological Applications* (Springer US, 1999).
- Béguin, F. & Frackowiak, E. *Supercapacitors: Materials, Systems, and Applications* (Wiley-VCH, 2013).
- Keskinen, J. et al. Architectural modifications for flexible supercapacitor performance optimization. *Electron. Mater. Lett.* **12**, 795–803 (2016).
- Kujala, M. et al. Screen printed vias for a flexible energy harvesting and storage module. In *2018 International Flexible Electronics Technology Conference, IFETC 2018* (2018).
- Park, J., Lee, J., Park, S., Shin, K. H. & Lee, D. Development of hybrid process for double-side flexible printed circuit boards using roll-to-roll gravure printing, via-hole printing, and electroless plating. *Int. J. Adv. Manuf. Technol.* **82**, 1921–1931 (2016).
- Shi, C. W. P. et al. Fabrication of wireless sensors on flexible film using screen printing and via filling. *Microsyst. Technol.* **17**, 661–667 (2011).
- Péter, M. et al. Reliable filling of through vias with silver based conductive adhesives in flexible PEN substrates using low-cost optimized stencil printing methods. In *2013 European Microelectronics Packaging Conference (EMPC)* 1–6 (2013).
- Park, J., Lee, J., Park, S. & Shin, K.-H., D. L. Development of hybrid process for double-side flexible printed circuit boards using roll-to-roll gravure printing, via-hole printing, and electroless plating. *Int. J. Adv. Manuf. Technol.* **82**, 1921–1931 (2016).
- Kramer, S. Printed Circuit Design & Manufacture, <https://www.thefreelibrary.com/Printed+Circuit+Design+%26+Manufacture/2004/March/1-p5327> (2004). Accessed 18 June 2020.
- Lorenz, E., Niemann, N., Koyuncu, M. & Bock, K. Reliability characterization of blind-hole vias for a System-in-Foil. In *Proceedings of the 5th Electronics System-Integration Technology Conference (ESTC)* 1–6 (IEEE, 2014).
- Harris, K. D., Elias, A. L. & Chung, H.-J. Flexible electronics under strain: a review of mechanical characterization and durability enhancement strategies. *J. Mater. Sci.* **51**, 2771–2805 (2016).
- Han, Y. & Dong, J. Electrohydrodynamic (EHD) Printing of Molten Metal Ink for Flexible and Stretchable Conductor with Self-Healing Capability. *Adv. Mater. Technol.* **3**, 1700268 (2018).
- Keskinen, J. et al. Lifetime and reliability of flexible aqueous supercapacitors: Constant voltage floating and bending experiments. In *2018 7th Electronic System-Integration Technology Conference, ESTC 2018 - Proceedings* (2018).
- Lehtimäki, S. et al. Performance, stability and operation voltage optimization of screen-printed aqueous supercapacitors. *Sci. Rep.* **7**, 46001 (2017).
- Hälonen, E. et al. Dynamic bending test analysis of inkjet-printed conductors on flexible substrates. In *Proceedings - Electronic Components and Technology Conference* 80–85 (2012).

## ACKNOWLEDGEMENTS

This work was partially funded by Business Finland as a part of the Towards Digital Paradise project (decision no. 2742/31/2016). T.M.K. was supported by a postdoctoral research fellowship received from the Tampere University of Technology Foundation (2016–2018). M.M. is supported by the Academy of Finland (grant nos. 288945 and 319408). We thank Behnam Khorramdel, DSc. for his contribution related to the via cross section preparation.

## AUTHOR CONTRIBUTIONS

M.K.: responsible for experiment sample preparation (i.e., screen-printing and bending study) and subsequent data collection. Data analysis and primary authorship of the paper. T.K.: responsible for laser processing and contributed to manuscript preparation. J.K.: contributed to data analysis, supercapacitor integration, and manuscript revisions. D.L.: contributed to manuscript review and supercapacitor case study. M.M.: contributed to design of experiment, data analysis, and manuscript authorship. T.M.K. is the corresponding author and responsible for design of experiment, as well as significant contributions to data analysis and authorship of the manuscript.



## COMPETING INTERESTS

The authors declare no competing interests.

## ADDITIONAL INFORMATION

**Supplementary information** is available for this paper at <https://doi.org/10.1038/s41528-020-00087-4>.

**Correspondence** and requests for materials should be addressed to T.M.K.

**Reprints and permission information** is available at <http://www.nature.com/reprints>

**Publisher's note** Springer Nature remains neutral with regard to jurisdictional claims in published maps and institutional affiliations.



**Open Access** This article is licensed under a Creative Commons Attribution 4.0 International License, which permits use, sharing, adaptation, distribution and reproduction in any medium or format, as long as you give appropriate credit to the original author(s) and the source, provide a link to the Creative Commons license, and indicate if changes were made. The images or other third party material in this article are included in the article's Creative Commons license, unless indicated otherwise in a credit line to the material. If material is not included in the article's Creative Commons license and your intended use is not permitted by statutory regulation or exceeds the permitted use, you will need to obtain permission directly from the copyright holder. To view a copy of this license, visit <http://creativecommons.org/licenses/by/4.0/>.

© The Author(s) 2020